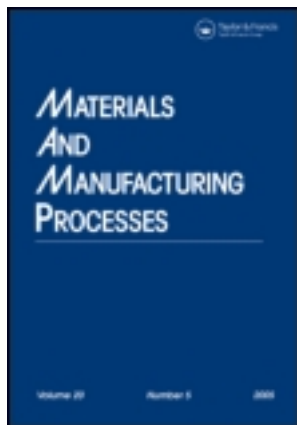


This article was downloaded by: [Central Electrochemical Res Inst]

On: 11 January 2012, At: 00:39

Publisher: Taylor & Francis

Informa Ltd Registered in England and Wales Registered Number: 1072954 Registered office: Mortimer House, 37-41 Mortimer Street, London W1T 3JH, UK



Materials and Manufacturing Processes

Publication details, including instructions for authors and subscription information:

<http://www.tandfonline.com/loi/lmmp20>

Low-Temperature Synthesis of Lithium Manganese Oxide Using LiCl-Li₂CO₃ and Manganese Acetate Eutectic Mixture

M. Helan^a & L. John Berchmans^b

^a Department of Chemistry, Jamal Mohamed College (Autonomous), Tiruchirappalli, Tamil Nadu, India

^b CSIR-CECRI-Electroprometallurgy Division, Central Electrochemical Research Institute, Karaikudi, Tamil Nadu, India

Available online: 24 May 2011

To cite this article: M. Helan & L. John Berchmans (2011): Low-Temperature Synthesis of Lithium Manganese Oxide Using LiCl-Li₂CO₃ and Manganese Acetate Eutectic Mixture, *Materials and Manufacturing Processes*, 26:11, 1369-1373

To link to this article: <http://dx.doi.org/10.1080/10426914.2010.536932>

PLEASE SCROLL DOWN FOR ARTICLE

Full terms and conditions of use: <http://www.tandfonline.com/page/terms-and-conditions>

This article may be used for research, teaching, and private study purposes. Any substantial or systematic reproduction, redistribution, reselling, loan, sub-licensing, systematic supply, or distribution in any form to anyone is expressly forbidden.

The publisher does not give any warranty express or implied or make any representation that the contents will be complete or accurate or up to date. The accuracy of any instructions, formulae, and drug doses should be independently verified with primary sources. The publisher shall not be liable for any loss, actions, claims, proceedings, demand, or costs or damages whatsoever or howsoever caused arising directly or indirectly in connection with or arising out of the use of this material.

Low-Temperature Synthesis of Lithium Manganese Oxide Using LiCl-Li₂CO₃ and Manganese Acetate Eutectic Mixture

M. HELAN¹ AND L. JOHN BERCHMANS²

¹Department of Chemistry, Jamal Mohamed College (Autonomous), Tiruchirappalli, Tamil Nadu, India

²CSIR-CECRI-Electrolytometallurgy Division, Central Electrochemical Research Institute, Karaikudi, Tamil Nadu, India

Fine crystalline LiMn₂O₄ powders have been prepared by molten salt synthesis (MSS) at 500°C, using an eutectic mixture of lithium chloride, lithium carbonate, and manganese acetate salts. Thermogravimetric and differential thermal analysis (TGA/DTA) measurements are performed to investigate the thermal decomposition behavior of the precursor salts. The single-phase cubic structure of LiMn₂O₄ is confirmed by X-ray powder diffraction analysis. The lattice parameter is found to be 8.1967 Å. The molecular structure of the compound is studied using FT-IR and Raman spectroscopy. The chemical composition and the purity of the synthesized powders are determined using atomic absorption spectroscopy (AAS), energy-dispersive X-ray spectroscopy (EDAX), and carbon hydrogen nitrogen sulfur (CHNS) analyses. The magnetic behavior of the compound is examined using electron paramagnetic resonance (EPR) spectroscopy. The morphology of the powders is assessed by scanning electron microscopy (SEM). The average particle size of the powders is ranging between 10–20 μm. This investigation shows that pure crystalline lithium manganese oxide powders can be conveniently synthesized by molten flux method.

Keywords Characterization; Diffusion; EPR; LiMn₂O₄; XRD.

INTRODUCTION

Rechargeable lithium-ion batteries have become a commercial reality in recent years. They are used in a multitude of mobile electronic equipments and transport systems. The global projections for the marketing of portable electronic devices with extraordinary capabilities create a driving force for the fabrication of an efficient, environmentally friendly and cheap rechargeable lithium-ion battery. Lithium cobaltate-LiCoO₂ is used as the cathode material in most of the commercial lithium batteries. However, the high cost and toxicity along with the safety problems have hindered the usage of LiCoO₂ in large-scale applications. In recent years, considerable efforts have focused on the development of alternate cathode materials to replace LiCoO₂. Lithium manganate-LiMn₂O₄ is one of the candidate materials, which crystallizes in the spinel structure with the space group of Fd3m. The oxygen atoms form a cubic-close packed array in which the Li atoms occupy one-eighth of the 8a tetrahedral sites and the Mn atoms occupy half of the 16d octahedral sites. The unoccupied 16c sites form a three dimensional network that facilitates the transport of Li⁺ cations [1].

Various methods have been tried to synthesise LiMn₂O₄ powders. It is reported that the preparation of pure crystals of LiMn₂O₄ is found to be difficult below 700°C using conventional solid-state method. It involves repeated crushing-calcining cycles to obtain pure phase of LiMn₂O₄ compound [2, 3]. It also consumes a large

amount of energy and the powders have relatively irregular morphology. In recent years, attention is focused on the development of a simple and reproducible low temperature synthesis route. Wet chemical methods such as co-precipitation [4], modified citrate gel process [5], and hydrothermal method [6] have been attempted to synthesize this compound. These methods need high temperature calcination and special autoclaves to achieve required properties. The above-mentioned difficulties induced us to explore new routes for the bulk-preparation of LiMn₂O₄ powders.

Molten salt synthesis (MSS) provides a way to overcome these problems that can result in the formation of stoichiometric compounds with good control over the chemistry, purity, morphology etc., of the crystals. Recently, the molten salt (MS) method is widely used for the preparation of unitary oxides, electrode materials, and multicomponent oxides [7–16]. MSs such as LiCl, LiNO₃, Li₂SO₄, LiOH do not only act as solvents but also take part in the reaction [16–18].

Advantages of MSS are as follows: (1) the temperature of synthesis can be lowered and the duration of reaction can be reduced because of high diffusivities, strong dissolving capability, large interfacial tension, and quick crystallization process; (2) the molten medium facilitates a better reaction condition with a high ion concentration of reactants; and (3) by using this technique, the large furnaces can be replaced with small ones, which can reduce the capital cost of the process. It means that this method is ideally convenient for a large-scale production of materials [19–25].

In MSS generally, two reaction sequences are considered for the product formation. In the first case, the reactants are dissolved in the MS, followed by the formation of the product in the molten medium and finally precipitate the

Received July 30, 2009; Accepted October 30, 2010

Address correspondence to L. John Berchmans, Scientist, Electrolytometallurgy Division, Central Electrochemical Research Institute, Karaikudi, Tamil Nadu 630006, India; E-mail: ljberchmans@gmail.com

product above its solubility limit. In the second case, one of the reactants dissolves in the MS and the dissolving component is transported to the outer surface of the other reactant and the product is formed on the latter surface [26, 27].

Tang et al. have tried the "Li-containing flux method" to prepare lithium manganese oxides, using LiCl-MnOOH salts [16]. Fine crystals of LiMn_2O_4 were synthesized using LiCl as the flux [28]. Spinel-type lithium manganese oxides were prepared at 400°C using LiNO_3 , $\gamma\text{-MnOOH}$, $\beta\text{-MnO}_2$, and birnessite ($\text{Na}_{0.3}\text{Ca}_{0.1}\text{K}_{0.1}$) $(\text{Mn}^{4+}, \text{Mn}^{3+})_2\text{O}_4 \cdot 1.5\text{H}_2\text{O}$ as the precursors [21].

In our previous communications, we reported the synthesis of LiMn_2O_4 and $\text{LiSm}_{0.01}\text{Mn}_{1.99}\text{O}_4$ compounds using LiCl-MnO₂ and LiCl-MnO₂-SmCl₃ · 6 · H₂O as the precursor salts [29, 30]. In the present work, we have made an attempt to synthesize this compound using manganese acetate ($\text{Mn}(\text{CH}_3\text{COO})_2 \cdot 4\text{H}_2\text{O}$) as one of the precursor salts with 0.6M LiCl and 0.4M Li₂CO₃ as the eutectic mixture. Various characterization techniques such as thermogravimetric and differential thermal analysis (TGA/DTA), X-ray diffraction (XRD), Fourier transform infrared (FT-IR), atomic absorption spectroscopy (AAS), CHNS, EDAX, electron paramagnetic resonance (EPR), and scanning electron microscopy (SEM) were used to identify the synthesized compound. The results on our investigation are presented in this article.

EXPERIMENTAL

LiMn_2O_4 powders were synthesized using high purity LiCl and Li₂CO₃ (99% purity, Merck) salts in the molar ratio of 0.6:0.4 (eutectic mixture) with Mn-acetate salt (98% purity, Aldrich). The molar ratio of the eutectic mixture and the transition metal acetate was fixed at 1:2. The chloride, carbonate, and acetate salts were ground using a mortar and pestle. Then the mixed salts were dried at 110°C for 8h. The dried powders were placed in a high-density alumina crucible and then heated in a muffle furnace at 500°C for 5h. The resulting mass was then cooled to ambient temperature. The residual flux was removed from the product by washing with 1M acetic acid followed by triple distilled water and dried at 120°C for 2h.

The thermal behavior of the precursor salts was studied by differential thermal analysis (DTA) and thermogravimetric analysis (TGA) using a thermal analyzer (model number STA 1500 PL Thermal Sciences, version V4.30 analyzer). The TGA/DTA curves were recorded from room temperature to 1000°C in air at a heating rate of 10°C/min. The purified product was characterized by XRD using philips 8030 X-ray diffractometer. The unit cell lattice parameters were determined using least-square fitting method of the d spacing and the hkl values. FT-IR spectroscopy was used to study the structure coordination of the calcined powders using Perkin Elmer UK paragon-500 spectrometer. To record the spectra, each sample was mixed with KBr and thoroughly ground in to fine powder and examined in the wave number ranging between 400–4000cm⁻¹. Raman spectral analysis was performed using a Renishaw InVia Microscope. The Raman system is equipped with a charge-coupled device (CCD) detector,

which gives the best spectral data. AAS analysis was done using a spectrophotometer (Varian Spectra 220). CHNS analysis was carried out using an instrument Elementar Vario EL III-Germany make. EPR was done using a Bruker Bio Spin GmbH EPR spectrometer. The measurement was performed at microwave frequency 9.857403GHz with fields corresponding to about 6500.000G sweep width. The morphology and the elemental composition of the synthesized powders were determined using a scanning electron microscope JEOL-JSM-3.5 CF-Japan make fitted with the EDAX facility.

RESULTS AND DISCUSSION

Figure 1 shows the TGA and DTA curves for the precursor salts on the synthesis of LiMn_2O_4 . The TGA curve exhibits four distinct weight loss steps. The first weight loss occurs between 81.01°C to 151.86°C is ascribed to the dehydration of water molecules. The loss in weight between 151.86°C to 266.58°C is mainly due to the decomposition of carbonate and acetate salts. The weight loss between 266.58°C and 372.30°C shows a sharp incursion, which is mainly due to the transformation of reactants into the product. The final weight loss of about 2.63wt% is noticed from 372.30°C to 1000°C, and is attributed to the evaporation of the melt at high temperature zone. The endothermic peak noticed at 136.12°C, is due to the evaporation of water molecules. The exothermic peak at 248.18°C is assigned to the decomposition of carbonate and acetate salts. A sharp exothermic peak at 369.48°C indicates the initiation of the compound formation.

The XRD spectrum of LiMn_2O_4 sample is presented in Fig. 2. All the XRD peaks are indexed for cubic structure of LiMn_2O_4 (space group: $\text{Fd}\bar{3}\text{m}-\text{O}_h^7$). The lattice constant value is determined by an iterative least-square refinement using "h, k, l" values. The lattice constant value for the cubic system $a = 8.1967 \text{ \AA}$ (JCPDS data card no. 88-1026), which is in good agreement with the reported value [31].

The FT-IR spectrum of LiMn_2O_4 synthesized at 500°C is shown in Fig. 3. The high-frequency bands, located around 610 and 519cm⁻¹ are associated with the asymmetric stretching modes of the MnO₆ group [32–35]. It is reported that the resonant frequencies of alkali metal cations in their

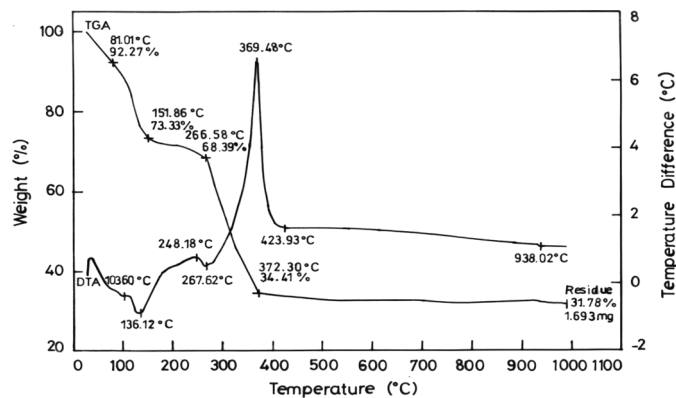


FIGURE 1.—TGA and DTA curves for LiMn_2O_4 synthesized by molten salt route.

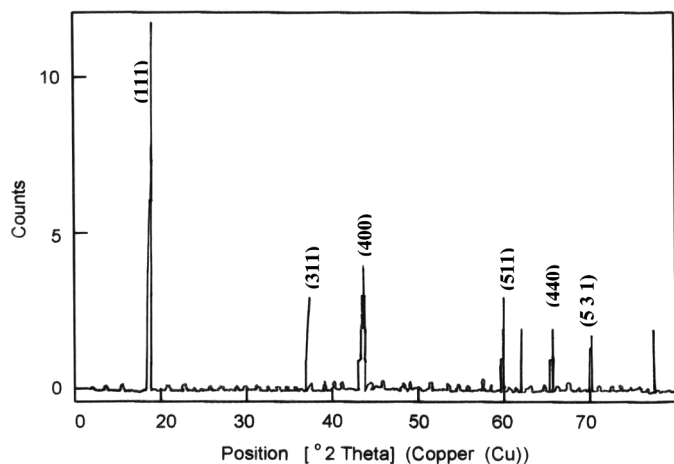


FIGURE 2.—X-ray powder diffraction pattern of the LiMn_2O_4 .

octahedral interstices (LiO_6) in inorganic oxides are located in the frequency range of $200\text{--}400\text{ cm}^{-1}$. The present study is restricted to the assignment of various vibrational modes of transition metal oxides within the frequency range of $400\text{--}1000\text{ cm}^{-1}$. These observations are quite similar to those given in earlier reports [36, 37].

Figure 4 shows the Raman spectrum of LiMn_2O_4 powders measured between $100\text{--}1000\text{ cm}^{-1}$. The spectrum mainly consists of strong bands between $600\text{--}700\text{ cm}^{-1}$ and several weak bands in the range of $150\text{--}400\text{ cm}^{-1}$. The strong band located at 662 cm^{-1} may be assigned to A_{1g} mode, corresponding to the symmetric Mn-O stretching vibration of MnO_6 groups. The weak bands may be assigned to three modes of t_{2g} phonons as reported in the literature. Further analysis of the spectrum is found to be complicated and the assignments are difficult to predict, since they are sensitive to the laser excitation [33, 38–40].

The concentration of Li and Mn ions is determined by AAS. An aliquot quantity of the sample is dissolved in 1N HCl solution, and the concentrations of Li and Mn ions are assessed. The determined values are presented in Table 1. It is found that the concentrations of Li and Mn ions

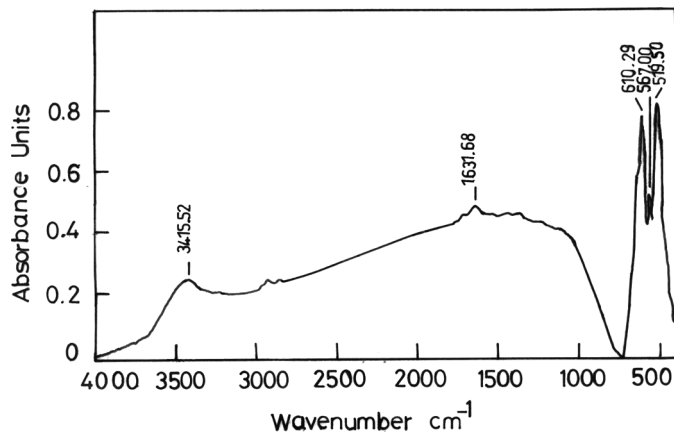


FIGURE 3.—FT-IR spectrum of LiMn_2O_4 .

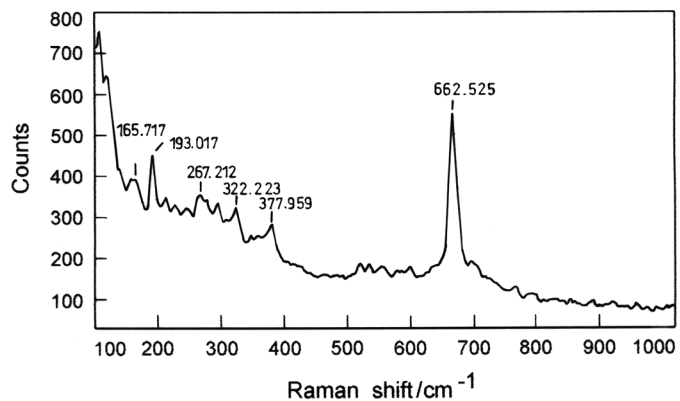


FIGURE 4.—Laser Raman spectrum of LiMn_2O_4 .

TABLE 1.—Atomic absorption spectroscopy (AAS) analysis of synthesized LiMn_2O_4 product.

Concentration of Lithium (%)	Concentration of Manganese (%)
3.1	58.77

TABLE 2.—Chemical analysis of synthesized LiMn_2O_4 product.

Compound	C	H	N	S
LiMn_2O_4	0.191	0.030	0.025	0.000

are in stoichiometric ratio, which confirms the compound LiMn_2O_4 . These values are in good agreement with the reported data [28].

The results on CHNS analysis are given in Table 2. From the table, it is noticed that the compound has minor impurities such as C, N, and H.

Figure 5 shows the EDAX profile of the synthesized LiMn_2O_4 compound. The EDAX spectrum shows the wt% of Mn and O in the product. The values are shown in Table 3. The results reveal that the absence of other impurities in the product.

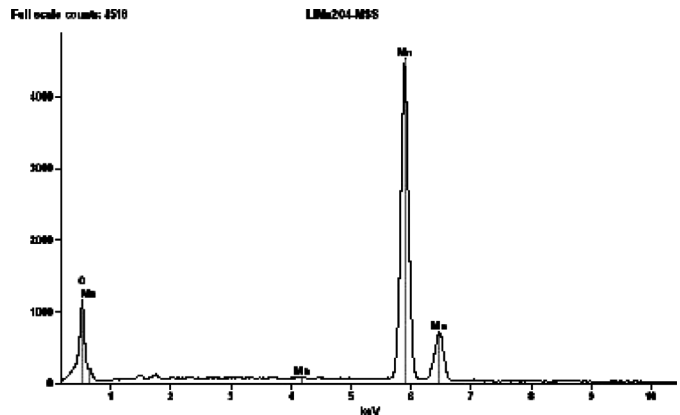


FIGURE 5.—EDAX profile of synthesized LiMn_2O_4 .

TABLE 3.—EDAX analysis of synthesized LiMn_2O_4 product.

Weight of Oxygen (%)	Weight of Manganese (%)
23.06	76.94

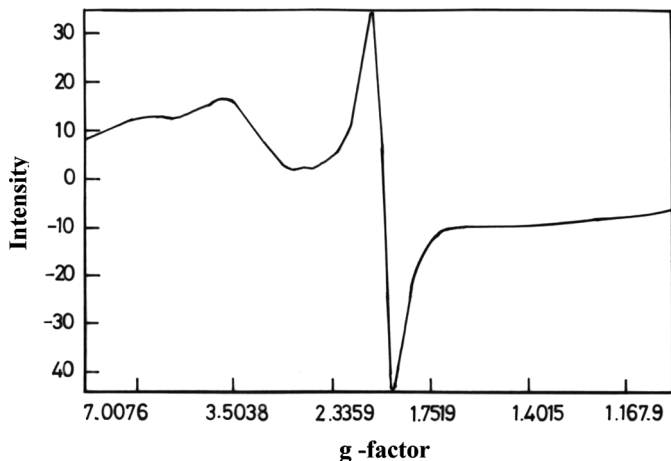
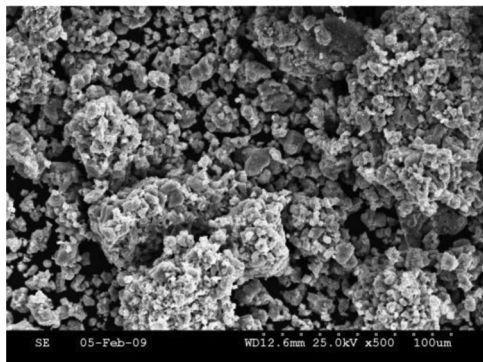
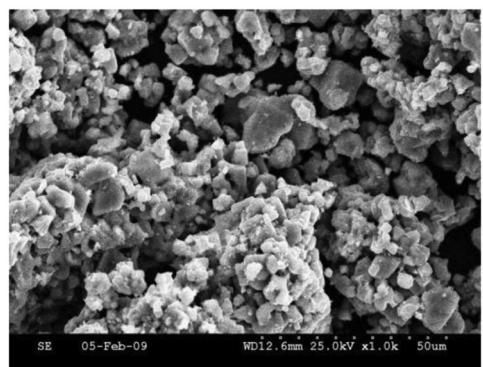


FIGURE 6.—EPR spectrum of LiMn_2O_4 .



(a)



(b)

FIGURE 7.—SEM micrographs of synthesized LiMn_2O_4 at different magnifications.

The paramagnetic behavior of the synthesized LiMn_2O_4 is determined using EPR studies. The EPR spectrum is shown in Fig. 6. It is noticed that the value of g factor is found to be 1.88, which is in good agreement with the reported value for LiMn_2O_4 . The Mn^{4+} - Mn^{4+} as well as the Mn^{4+} - Mn^{3+} dipolar interactions are responsible for the broadening of the signal. The EPR signal corresponds to the collective motion of the total magnetic moment of the Mn^{3+} and Mn^{4+} spin system [41–43].

The scanning electron micrographs of LiMn_2O_4 powders are shown in Fig. 7(a) and (b). The particle morphology is dominated by the nucleation and growth process. The SEM images reveal that the particles have assorted morphology with the average particle size of 10–20 μm .

CONCLUSIONS

Pure fine crystalline LiMn_2O_4 powders were synthesized using MS method. The XRD data confirm the cubic spinel structure of the compound with lattice constant value $a = 8.1967 \text{ \AA}$. FT-IR spectrum reveals the high-frequency bands, located around 610 and 519 cm^{-1} , are associated with the asymmetric stretching modes of the MnO_6 group. Raman spectrum shows a strong band located at 662 cm^{-1} may be assigned to A_{1g} mode, responsible for the symmetric Mn-O stretching vibration of MnO_6 groups. The EPR spectrum shows a broad signal at $g = 1.88$ and corresponds to the collective motion of the total magnetic moment of the Mn^{3+} and Mn^{4+} spin system. From the above investigation, it has been concluded that pure phase of Li-Manganese oxide powders can be easily prepared using simple salts by the low-temperature MSS route.

ACKNOWLEDGMENTS

The authors sincerely thank the Director, CECRI, for his kind permission and the staff of Electroprometallurgy Division for their support and encouragement to carry out this study.

REFERENCES

- Bao, S.J.; Liang, Y.Y.; Zhou, W.J.; He, B.L.; Li, H.L. Synthesis and electrochemical properties of $\text{LiAl}_{0.1}\text{Mn}_{1.9}\text{O}_4$ by microwave-assisted sol-gel method. *J. Power Sources* **2006**, *154*, 239–245.
- Massarotti, V.; Capsoni, D.; Bini, M. Nanosized LiMn_2O_4 from mechanically activated solid-state synthesis. *J. Solid State Chem.* **2006**, *179*, 590–596.
- Wan, C.; Nuli, Y.; Zhuang, J.; Jiang, Z. Synthesis of spinel LiMn_2O_4 using direct solid state reaction. *Mater. Lett.* **2002**, *56*, 357–363.
- Chan, H.W.; Duh, J.G.; Sheen, S.R. LiMn_2O_4 cathode doped with excess lithium and synthesized by co-precipitation for Li-ion batteries. *J. Power Sources* **2003**, *115*, 110–118.
- Hwang, B.J.; Santhanam, R.; Liu, D.G. Characterization of nanoparticles of LiMn_2O_4 synthesized by citric acid sol-gel method. *J. Power Sources* **2001**, *97–98*, 443–446.
- Wu, H.M.; Tu, J.P.; Yuan, Y.F.; Chen, X.T.; Xiang, J.Y.; Zhao, X.B.; Cao, G.S. One-step synthesis LiMn_2O_4 cathode by a hydrothermal method. *J. Power Sources* **2006**, *161*, 1260–1263.
- Duran, C.; Messing, G.L.; McKinstry, S.T. Molten salt synthesis of anisometric particles in the $\text{SrO-Nb}_2\text{O}_5\text{-BaO}$ system. *Mater. Res. Bull.* **2004**, *39*, 1679–1689.

8. Harle, V.; Vrinat, M.; Scharff, J.P.; Durand, B.; Deloume, J.P. Catalysis assisted characterizations of nanosized $\text{TiO}_2\text{-Al}_2\text{O}_3$ mixtures obtained in molten alkali metal nitrates: Effect of the metal precursor. *Appl. Catal. A: Gen.* **2000**, *196*, 261–269.
9. Xu, C.K.; Zhao, X.L.; Liu, S.; Wang, G.H. Large-scale synthesis of rutile SnO_2 nanorods. *Solid. State. Commun.* **2003**, *125*, 301–304.
10. Gorokhovskiy, A.V.; Escalante-Garc, J.I.; Sanchez-Monjaras, T.; Gutierrez-Chavarria, C.A. Synthesis of potassium polytitanate precursors by treatment of TiO_2 with molten mixtures of KNO_3 and KOH . *J. Eur. Ceram. Soc.* **2004**, *24*, 3541–3546.
11. Docters, T.; Chovelon, J.M.; Herrmann, J.M.; Deloume, J.P. Syntheses of TiO_2 photocatalysts by the molten salts method: Application to the photocatalytic degradation of Prosulfuron. *Appl. Catal. B: Environ.* **2004**, *50*, 219–226.
12. Liang, H.; Qiu, X.; Chen, H.; He, Z.; Zhu, W.; Chen, L. Analysis of high rate performance of nanoparticled lithium cobalt oxides prepared in molten KNO_3 for rechargeable lithium-ion batteries. *Electrochem. Commun.* **2004**, *6*, 789–794.
13. Kim, J.H.; Myung, S.T.; Sun, Y.K. Molten salt synthesis of $\text{LiNi}_{0.5}\text{Mn}_{1.5}\text{O}_4$ spinel for 5V class cathode material of Li-ion secondary battery. *Electrochim. Acta*, **2004**, *49*, 219–227.
14. Tan, K.S.; Reddy, M.V.; Subba Rao, G.V.; Chowdari, B.V.R. High-performance LiCoO_2 by molten salt ($\text{LiNO}_3\text{:LiCl}$) synthesis for Li-ion batteries. *J. Power Sources* **2005**, *147*, 241–248.
15. Liang, H.Y.; Qiu, X.P.; Zhang, S.C.; He, Z.Q.; Zhu, W.T.; Chen, L.Q. High performance lithium cobalt oxides prepared in molten KCl for rechargeable lithium-ion batteries. *Electrochem. Commun.* **2004**, *6*, 505–509.
16. Yang, X.Y.; Tang, W.P.; Kanoh, H.; Ooi, K. Synthesis of lithium manganese oxide in different lithium-containing fluxes. *J. Mater. Chem.* **1999**, *9*, 2683–2690.
17. Chiu, C.C.; Li, C.C.; Desu, S.B. Molten salt synthesis of a complex perovskite, $\text{Pb}(\text{Fe}_{0.5}\text{Nb}_{0.5})\text{O}_3$. *J. Am. Ceram. Soc.* **1991**, *74*, 38–41.
18. Yoon, K.H.; Cho, Y.S.; Lee, D.H.; Kang, D.H. Powder characteristics of $\text{Pb}(\text{Mg}_{1/3}\text{Nb}_{2/3})\text{O}_3$ prepared by molten salt synthesis. *J. Am. Ceram. Soc.* **1993**, *76*, 1373–1376.
19. Arent, R.H.; Rosolowski, Z.H.; Szymaszek, J.W. Lead zirconate titanate ceramics from molten salt solvent synthesized powders. *Mater. Res. Bull.* **1979**, *14*, 703–709.
20. Xu, R.; Pang, W. *Inorganic Synthesis and Preparation Chemistry*; Higher Education Press: Beijing, 2001.
21. Yang, X.J.; Tang, W.P.; Liu, Z.H.; Makita, Y.; Ooi, K. Synthesis of lithium-rich $\text{Li}_x\text{Mn}_2\text{O}_4$ spinels by lithiation and heat-treatment of defective spinels. *J. Mater. Chem.* **2002**, *12*, 489–495.
22. McCarthy, T.J.; Kanatzidis, M.G. Use of molten alkali-metal polythiophosphate fluxes for synthesis at intermediate temperatures. Isolation and structural characterization of ABiP_2S_7 ($A = \text{K, Rb}$). *Chem. Mater.* **1993**, *5*, 1061–1063.
23. Thirumal, M.; Ganguli, A.K. Phase analysis and dielectric properties of ceramics in $\text{PbO-MgO-ZnO-Nb}_2\text{O}_5$ system: A comparative study of materials obtained by ceramic and molten salt synthesis routes. *Bull. Mater. Sci.* **2000**, *23*, 255–261.
24. Zhu, L.H.; Huang, Q.W.; Gu, H. Preparation of acicular strontium barium potassium niobate seed crystals. *J. Cryst. Growth*, **2004**, *267*, 199–203.
25. Lin, Y.; Yang, H.; Zhu, J.; Wang, F.; Luo, H. Low-temperature rapid synthesis of LiNbO_3 powders by molten salt methods. *Materials and Manufacturing Processes* **2008**, *23*, 791–795.
26. Yoon, K.H.; Cho, Y.S.; Kang, D.H. Molten salt synthesis of lead-based relaxors. *J. Mater. Sci.* **1998**, *33*, 2977–2984.
27. Zhang, S.; Jayaseelan, D.D.; Bhattacharya, G.; Lee, W.E. Molten salt synthesis of magnesium aluminate (MgAl_2O_4) spinel powder. *J. Am. Ceram. Soc.* **2006**, *89*, 1724–1726.
28. Tang, W.; Yang, X.; Liu, Z.; Kasaishi, S.; Ooi, K. Preparation of fine single crystals of spinel-type lithium manganese oxide by LiCl flux method for rechargeable lithium batteries. Part 1: LiMn_2O_4 . *J. Mater. Chem.* **2002**, *12*, 2991–2997.
29. Helan, M.; Berchmans, L.J.; Hussain, A.Z. Synthesis of LiMn_2O_4 by molten salt technique. *Ionics* **2010**, *16*, 227–231.
30. Helan, M.; Berchmans, L.J. Synthesis of $\text{LiSm}_{0.01}\text{Mn}_{1.99}\text{O}_4$ by molten salt technique. *J. Rare Earths* **2010**, *28*, 225–259.
31. Du, K.; Zhang, H. Preparation and performance of spinel LiMn_2O_4 by a citrate route with combustion. *J. Alloy. Comp.* **2003**, *352*, 250–254.
32. Kalyani, P.; Kalaiselvi, N.; Muniyandi, N. A new solution combustion route to synthesize LiCoO_2 and LiMn_2O_4 . *J. Power Sources* **2002**, *111*, 232–238.
33. Amundsen, B.; Burns, G.R.; Islam, M.S.; Kanoh, H.; Roziere, J. Lattice dynamics and vibrational spectra of lithium manganese oxides: A computer simulation and spectroscopic study. *J. Phys. Chem B.* **1999**, *103*, 5175–5180.
34. Rouier, A.; Nazri, G.A.; Julien, C. Vibrational spectroscopy and electrochemical properties of $\text{LiNi}_{0.7}\text{Co}_{0.3}\text{O}_2$ cathode material for rechargeable lithium batteries. *Ionics* **1997**, *3*, 170–176.
35. Raja, M.W.; Mahanty, S.; Paromita, G.; Basu, R.N.; Maiti H.S. Alanine-assisted low-temperature combustion synthesis of nanocrystalline LiMn_2O_4 for lithium-ion batteries. *Mater. Res. Bull.* **2007**, *42*, 1499–1506.
36. Richardson, T.J.; Ross, P.N. Jr. FTIR spectroscopy of metal oxide insertion electrodes: Thermally induced phase transitions in $\text{Li}_x\text{Mn}_2\text{O}_4$ spinels. *Mater. Res. Bull.* **1996**, *31*, 935–941.
37. Preudhomme, J.; Tarte, P. Infrared studies of spinels—III: The normal II–III spinels. *Spectrochim. Acta* **1971**, *27*, 1817–1835.
38. Chitra, S.; Kalyani, P.; Mohan, T.; Massot, M.; Ziolkiewicz, S.; Gangandharan, R.; Eddrief, M.; Julien, C. Physical properties of LiMn_2O_4 spinel prepared at moderate temperature. *Ionics* **1998**, *4*, 8–15.
39. Palone, A.; Sacchetti, A.; Corridoni, T.; Postorino, P.; Cantelli, R. MicroRaman spectroscopy on LiMn_2O_4 : Warnings on laser-induced thermal decomposition. *Solid State Ionics* **2004**, *170*, 135–138.
40. Tang, S.B.; Lai, M.O.; Lu, L.; Tripathy, S. Comparative study of LiMn_2O_4 thin film cathode grown at high, medium and low temperatures by pulsed laser deposition. *J. Solid State Chem.* **2006**, *179*, 3831–3838.
41. Caponi, D.; Bini, M.; Chiodelli, G.; Massarotti, V.; Mozzatti, M. C.; Anzoni, C. Structural transition in Mg-doped LiMn_2O_4 : A comparison with other M-doped Li–Mn spinels. *Solid State Commun.* **2003**, *125*, 179–183.
42. Amdouni, N.; Zaghbi, K.; Gendron, F.; Mauger, A.; Julien, C.M. Magnetic properties of $\text{LiNi}_{0.5}\text{Mn}_{1.5}\text{O}_4$ spinels prepared by wet chemical methods. *J. Magn. Magn. Mater.* **2007**, *309*, 100–105.
43. Stoyanova, R.; Gorova, M.; Zhecheva, E. EPR of Mn^{4+} in spinels $\text{Li}_{1+x}\text{Mn}_{2-x}\text{O}_4$ with $0 \leq x \leq 0.1$. *J. Phys. Chem. Solids* **2000**, *61*, 609–614.